

Interplay between Zika virus-induced autophagy and neural stem cell fate determination

Bindu .

National Brain Research Centre

Hriday Shanker Pandey

National Brain Research Centre

Pankaj Seth (✉ pseth.nbrc@gov.in)

National Brain Research Centre <https://orcid.org/0000-0003-1021-7839>

Research Article

Keywords: ZIKA, Microcephaly, Mitochondrial fission, Notch, ROS

Posted Date: April 20th, 2023

DOI: <https://doi.org/10.21203/rs.3.rs-2817082/v1>

License: © ⓘ This work is licensed under a Creative Commons Attribution 4.0 International License.

[Read Full License](#)

Version of Record: A version of this preprint was published at Molecular Neurobiology on November 1st, 2023. See the published version at <https://doi.org/10.1007/s12035-023-03704-1>.

Abstract

The Zika virus (ZIKV) outbreaks and its co-relation with microcephaly have become a global health concern. It is primarily transmitted by a mosquito, but can also be transmitted from an infected mother to her fetus causing impairment in brain development, leading to microcephaly. However, the underlying molecular mechanism of ZIKV-induced microcephaly is poorly understood. In this study, we explored the role of ZIKV non-structural protein NS4A and NS4B in ZIKV pathogenesis in a well-characterized primary culture of human fetal neural stem cells (fNSCs). We observed that the co-transfection of NS4A and NS4B altered the neural stem cell fate by arresting proliferation and inducing premature neurogenesis. NS4A-NS4B transfection in fNSCs increased autophagy and dysregulated notch signalling. Further, it also altered the regulation of downstream genes controlling cell proliferation. Additionally, we reported that 3 methyl-adenine (3MA), a potent autophagy inhibitor, attenuated the deleterious effects of NS4A and NS4B as evidenced by the rescue in Notch1 expression, enhanced proliferation, and reduced premature neurogenesis. Our attempts to understand the mechanism of autophagy induction indicate the involvement of mitochondrial fission and ROS. Collectively, our findings highlight the novel role of NS4A and NS4B in mediating NSC fate alteration through autophagy-mediated notch degradation. The study also helps to advance our understanding of ZIKV-induced neuropathogenesis and suggests autophagy as a potential target for anti-ZIKV therapeutic intervention.

Introduction

Zika virus (ZIKV) is a mosquito-borne virus (arbovirus) initially discovered in Uganda but now has a worldwide presence [1]. It belongs to the Flavivirus genus in the Flaviviridae family. Its 10.7 kb positive-sense RNA genome encodes a single polyprotein which is cleaved to 3 structural protein capsid (C), pre-membrane (prM), and envelope (E), and seven non-structural proteins consisting of NS1, NS2A, NS2B, NS3, NS4A, NS4B, and NS5 [2]. It is primarily transmitted by the vector *Aedes* mosquitoes (*Aedes aegypti*, *Aedes luteocephalus*, and *Aedes albopictus*) but non-vector transmittance like transplacental transmittance from mother to baby is also reported [3]. In recent outbreaks, ZIKV is associated with inducing microcephaly [4]. ZIKV also causes other neurological disorders like myelitis, encephalitis, and Guillain-Barré syndrome apart from causing microcephaly [5–7]. Congenital Zika Syndrome (CZS) is currently recognized as the most severe effect of ZIKV, which is characterized by microcephaly and other neurological problems due to intrauterine infection [8]. As ZIKV is a global health risk, its associated neurological problems necessitate a clear understanding of ZIKV-induced neuropathogenesis that may help in designing therapeutic interventions.

Microcephaly is a neurodevelopmental disorder characterized by reduced brain size, intellectual disability, motor disorder, vision or auditory problems, and language disabilities [9–11]. Findings from several clinical and epidemiological investigations report a causal link between ZIKV and microcephaly [8]. Neural stem cells (NSCs) are key targets of ZIKV and the altered cell cycle regulation in these cells leading to reduced proliferation and impaired neurogenesis is linked to microcephaly induction [1, 12]. The impaired proliferation of NSCs was reported in ZIKV-infected culture models and organoids [13–15] and

during brain development in ZIKV-infected mice [16–19]. Some reports show that the ZIKV infection leads to abnormal centriole–spindle arrangements and chromosomal abnormalities [8]. Increased cell death and autophagy are also observed in several infection models along with reduced cell proliferation and impairment of neurogenesis [13–15, 20–23]. However, the mechanistic understanding of ZIKV effects on NSC fate determination remains unclear.

Flaviviruses such as Dengue virus (DENV) and Hepatitis C virus (HCV) manipulate autophagy to enhance their replication [24]. Interestingly, ZIKV protein NS4A and NS4B downregulate AKT-mTOR signaling to induce autophagy [23]. Autophagy is a fundamental process having regulatory and protective roles. It regulates several cell signaling pathways to control cell fate. It has also been reported that the notch receptor and its cleaved form (NICD) is one of the targets of autophagy and gets degraded through it [24]. The notch signaling pathway is critical for maintaining homeostasis between NSC proliferation and neurogenesis [25]. Surprisingly, the detailed mechanisms of how ZIKV proteins affect these fundamental processes and impact NSC cell fate, remain poorly understood. These lacunae in the field necessitated this study.

In our study, we employed well-characterized primary cultures of human fetal brain-derived neural stem cells (fNSCs) to study if overexpression of NS4A and NS4B, the two important non-structural proteins of ZIKV, in human NSCs, alter their properties of proliferation and differentiation, and also to gain novel insights into the molecular mechanisms of ZIKV induced neuropathogenesis. We studied the markers of the autophagy pathways and carried out experiments using autophagy-targeted drugs to check if NSC proliferation and reduced neurogenesis could be reversed in fNSCs.

Results

Zika virus non-structural proteins NS4A and NS4B co-transfection reduces fetal neural stem cells proliferation and induces premature neurogenesis

Human fNSCs were isolated from the subventricular region of the aborted human fetus. More than 95% of these cells expressed Nestin and SOX2, well-known markers of NSCs, as evident from immunocytochemistry (Fig.S1). When grown in suspension culture, fNSCs proliferate and generate neurospheres. Hence, the size of the neurospheres represents the cell proliferating capability. Among the several ZIKV proteins, non-structural proteins 4A and 4B have been reported to have a significant effect on cell proliferation [26].

We confirmed these findings by transfecting the fetal neural stem cells (fNSCs) with ZIKA virus NS4A and NS4B expression vectors for 24 hours. We found that co-transfection of NS4A and NS4B significantly hampered cell proliferation as neurosphere size was found to be significantly reduced when compared to the vector control (Fig. 1a-b). In the vector control group, around 13% of the neurospheres formed were of small size ($\leq 50 \mu\text{m}$), and 45% were of large size ($\geq 100 \mu\text{m}$), whereas the percentage of small-size neurospheres and large-size neurospheres was around 24% and 29% respectively for the co-transfection group. Medium-size neurospheres (50–100 μm) were almost equal in both groups (Fig. 1b).

We also assayed cell proliferation by assessing the expression of the cell proliferation marker (Ki-67) using immunostaining. We observed that Ki-67 positive cells were reduced after NS4A and NS4B co-transfection (37% in vector control vs 16% in the NS4A + NS4B group) which supported the findings of our neurosphere assays (Fig. 1c-d).

Further, we checked the effect of these viral expression vectors on fNSC survival using TUNEL assay and found no significant change in TUNEL positive cell population in the co-transfection condition compared to the vector control (Fig. 1e-f). This suggests that Zika virus NS4A and NS4B expression vectors synergistically reduce fNSC proliferation without affecting their survival.

Since we observed reduced neural stem cell proliferation and no significant change in cell death, we further hypothesized that these cells might be undergoing premature differentiation resulting in the reduction of the pool of NSCs. Therefore, we evaluated neurogenesis in non-differentiating culture conditions by analyzing the transcriptional expression of NSC commitment markers (TBR2) and neurogenesis markers (DCX, PTN, ROBO). We found increased expression levels of ROBO, DCX, and TBR2 in the NS4A + NS4B co-transfection condition compared to the vector control, however no significant change in PTN was reported (Fig. 2a). We further analyzed the protein expression level of early neurogenesis markers such as DCX and TUJ1 by performing immunocytochemistry. We found around a 1.5-fold increase in DCX + cells and TUJ1 + cells in NS4A + NS4B transfected groups as compared to the vector control (Fig. 2b-e). We did not observe any significant change in (GFAP astrocyte marker) after the transfection. (Fig. S2). These results suggest that ZIKV NS4A and NS4B induce premature neurogenesis in fNSCs, but not gliogenesis.

Zikv Vectors Ns4a And Ns4b Induce Autophagy In FnsCs

The autophagy pathway is manipulated by different viruses such as Dengue virus, Poliovirus, and Hepatitis C virus for enhancing viral replication [27]. Zika virus is also found to alter the autophagy pathway in multiple cell types [26]. As autophagy is a key regulator of cellular homeostasis, we investigated the level of autophagy in our system.

We assessed autophagy key events following ZIKV NS4A and NS4B co-transfection by analyzing the transcriptional expression of several genes, such as ATG7, ATG13, ATG16L1, LAMP1, and LAMP2, involved at different steps of the autophagy pathway. We found a significant increase in transcript levels of *Atg13*, *Atg7*, *Atg16L1*, and *Lamp1* (Fig. 3A), involved in autophagy induction, autophagosome formation, and autophagosome maturation. This provided convincing evidence that NS4A and NS4B induced autophagy in human fNSCs, which may then alter the fate of neural stem cells.

LC3BII, which facilitates cargo recruitment, and p62, which are cargo receptors are frequently used as markers for evaluating autophagy [28]. We found a 1.8-fold increase in the level of LC3BII and found a marked reduction (around 40%) in the p62 level in the immunoblot assay after co-transfection of NS4A-NS4B (Fig. 3b-c). These results further demonstrated significant enhancement in the autophagy pathway

after transfection of ZIKV vectors mimicking ZIKV infection of NSCs. Therefore, autophagy appears to be a key mechanistic mediator for impaired fNSC proliferation and premature neurogenesis in ZIKV-induced neuropathogenesis.

Zikv Ns4a And Ns4b Impair Notch Signalling

It has also been reported that the notch receptor and its cleaved form (NICD) is one of the targets of autophagy and gets degraded through it [24]. Therefore, we assessed the status of the notch signaling pathway as it might be involved in this context. We found a 33% decrease in Notch1 protein expression after NS4A-NS4B expression compared to the vector control (Fig. 4a), representing the downregulation of the notch signaling. Autophagy also regulates Wnt signaling by degrading the Wnt receptor Dvl2 and importantly Wnt signaling is also associated with cell proliferation [29]. Hence, we also measured the expression of Dvl2 in NS4A-NS4B transfected human NSCs, but we did not observe any significant change in Dvl2 protein expression after transfection (Fig. 4b). Therefore, we focused the rest of the study on the characterization of the notch signaling regulation under the effect of ZIKV NS4A + NS4B.

Notch signaling alters neural stem cell proliferation by regulating the genes that induce proliferation, such as basic helix loop helix (BHLH) family genes (*Hes1*, *Hes5*, *Hey1*, and *Hey2*) which further suppresses NSCs differentiation by inhibiting pro-neurogenic genes (Neurogenin1, Neurogenin 2)[30]. We assessed the expression of these genes by performing quantitative PCR in the control and NS4A + NS4B transfected groups. We observed downregulation in *Hes1*, *Hes5*, and *Hey2* and upregulation in Neurogenin 1 and Neurogenin 2 transcript levels (Fig. 4c). This suggests the cells are undergoing premature neurogenesis instead of proliferation and changing their fate towards neurogenesis following co-transfection with ZIKV NS4A and NS4B expression vectors.

Autophagy Inhibition Restores The Zikv (Ns4a + ns4b)- Induced Molecular Imbalance

We found a significant molecular imbalance of neural stem cells after ZIKV NS4A-NS4B co-transfection and induction of autophagy. To further strengthen the observed effects in neural stem cells, we evaluated the effects of autophagy inhibitor 3-methyladenine (3-MA) on the NSCs expressing NS4A and NS4B. The 3-MA inhibits autophagy by blocking autophagosome formation via the inhibition of selective class III phosphatidylinositol 3-kinases [31]. We transfected the cells for 12h with an empty vector or a combination of NS4A and NS4B followed by 12 hours of 3-MA (3.5 μ M) treatment. This resulted in decreased LC3BII protein levels (Fig. 5a-b), indicating inhibition of autophagy induction in fNSCs after ZIKV transfection. We further analyzed the effect of 3-MA on Notch signaling in fNSCs after ZIKV transfection and observed that the NS4A-NS4B-induced decreased Notch1 protein (NICD) expression was rescued to a level comparable to the control group (Fig. 5a, c). These results indicate that inhibiting autophagy after NS4A-NS4B transfection restores the molecular signature of neural stem cells to the normal level. This also suggests inhibiting autophagy after NS4A-NS4B transfection might rescue the

impaired cell proliferation and premature neurogenesis phenotype of neural stem cells and offers a possible therapeutic window.

Autophagy Inhibition Restores Neural Stem Cell Proliferation And Inhibits Premature Neurogenesis

Further, we wanted to study the effects of autophagy inhibition on ZIKV (NS4A + NS4B)-induced phenotype viz NSC proliferation arrest and premature neurogenesis. We treated the NSCs with autophagy inhibitor 3-MA (3.5 μ M) for 12h after 12h of co-transfection with NS4A and NS4B and performed immunocytochemistry analysis for the Ki-67 cell proliferation marker. We found a significant increase in the Ki-67 positive cell population after 3-MA treatment in NS4A + NS4B transfected group compared to the untreated NS4A + NS4B transfected group (Fig. 6a-b). This suggests that 3-MA treatment enhances the proliferation in the transfected group. These results confirm that autophagy inhibition can rescue NSCs proliferation. We also performed immunocytochemistry for DCX to assess if there is a recovery in premature neurogenesis after 3-MA drug treatment and observed that 3-MA treatment decreased the expression of DCX to the control level in NS4A and NS4B co-transfection group (Fig. 6c-d). These results strongly suggest that regulated inhibition of autophagy might prevent ZIKV-associated neurodevelopmental abnormality.

Zikv Ns4a - Ns4b Co-transfection Altered Mitochondrial Dynamics

Mitochondrial dynamics regulate autophagy as well as neural stem cell fate by regulating redox balance [32] [33]. To understand the mechanisms driving the enhancement of the autophagy pathway, we investigated if mitochondrial dynamics is playing any role in autophagy induction.

To assess this, we co-transfected the NSCs with ZIKV NS4A and NS4B plasmids for 24h, isolated the protein and RNA, and performed quantitative PCR and immunoblotting for mitochondrial fusion (*Mfn1*, *Mfn2*, *Opa1*) and mitochondrial fission genes (*Drp1*). Although we found no significant change in *Mfn1*, *Mfn2*, and only 7% change in *Opa1*, the transcript level of *Drp1* was significantly increased (Fig. 7a). Similar results were observed when we performed immunoblotting with MFN2 and DRP1-specific antibodies. No significant change in MFN2 was reported, but DRP1 protein expression was significantly increased (45%) (Fig. 7b-e). These results indicate that ZIKV NS4A and NS4B enhance mitochondrial fission without altering mitochondrial fusion.

Mitochondria are the primary site of reactive oxygen species (ROS) production, and enhanced mitochondrial fission has been positively correlated with increased ROS production, on the other hand, ROS has been found to enhance the autophagy pathway by inhibiting the mTOR pathway [32]. Antioxidant treatment prevents autophagy, suggesting that redox imbalance has a crucial role in driving the process of autophagy [32]. So next, the level of ROS production was measured in the co-transfected cells and we found around a 30% increase in ROS production following NS4A and NS4B co-transfection

(Fig. 7f). These results clearly suggest that altered mitochondrial dynamics along with the associated unbalanced ROS production, may contribute to enhanced autophagy.

Discussion

Re-emergence of the zika virus is a global health concern as it is associated with a congenital developmental disorder like microcephaly [34]. Recent efforts to understand the impact of ZIKV infection on human brain development have revealed some key aspects of pathogenesis. Several *in vitro and in vivo* studies show that ZIKV preferentially infects neural stem cells/ progenitor cells and affects cell cycle regulation, differentiation, apoptosis, autophagy, and immune response [35]. ZIKV infection impairs fetal brain growth by arresting neuronal stem cell proliferation and inducing premature differentiation and such events lead to depletion in the neuronal progenitor cell pool [36]. Transcriptomics and *in silico* analysis also suggest several dysregulations in cellular and molecular processes in neural progenitor cells under the effect of ZIKV [35].

Neural stem cells are the primary targets of ZIKV, as reported by studies [15]. The mechanism behind the Zika virus hampering NSC proliferation is still not very clear hence hindering the development of Zika virus-targeted anti-viral therapy, especially for microcephaly. To decipher this, we used fNSCs as a model system to study the mechanism that may contribute to the neurodevelopmental disorders following exposure to ZIKV infections. As the ZIKV induced microcephaly is a developmental disorder, fNSC model is an apt model. We found that ZIKV NS4A and NS4B proteins hamper NSCs proliferation by altering autophagy-mediated notch degradation.

We first observed that co-transfection of ZIKV protein NS4A and NS4B hampered NSCs proliferation as was evident by neurosphere assay and Ki-67 labelling, this was in agreement with our earlier studies with ZIKV E- protein [20] as well as with previous reports by other groups [26]. The balance between neural stem cell maintenance and commitment is critical for normal brain development [37]. Genetic defects in neurogenesis and migration often result in developmental neurological disorders, including microcephaly. ZIKV directs the cells toward premature neurogenesis as observed by enhanced neurogenesis markers like DCX, and Tuj1, but not astrocytic marker GFAP. Premature neurogenesis is a hallmark of microcephaly [38]. Hence our findings strengthen the observation that ZIKV impairs neural stem/progenitor cell proliferation and fate determination.

Autophagy is a degradation system to degrade defective proteins or viruses or recycle amino acids. Although autophagy is a defence pathway of a cell to fight against pathogens, several flaviviruses utilize this pathway for their benefit. Recently its role in viral replication and neural stem cell proliferation has been studied [27] [39]. So, we hypothesized autophagy could be involved in the ZIKV-induced decrease in NSCs proliferation and carried out a detailed investigation of the autophagy pathway.

The autophagy process involves cascade of events regulated by several molecules. For instance, ATG13 is involved in autophagy induction, whereas ATG7 and ATG16L1 are involved in (LC3I-LC3II conversion) or autophagosome formation [39]. Lysosome-associated membrane protein-1 (LAMP-1) and LAMP-2 are

important protein components of the lysosomal membrane. They are involved in autophagosome maturation [40]. We observed that co-transfection of ZIKV NS4A and NS4B enhanced autophagy as shown by enhanced mRNA expression of the autophagy genes involved at different levels of autophagy. However, LAMP2 remained unaffected under the effect of viral expression vectors. During autophagy, cytosolic LC3BI is lipidated to form LC3BII, which associates with autophagosome membranes and facilitates the recruitment of cargo into the pathway; thus, an increase in the LC3B II level is indicative of autophagy induction. The levels of SQSTM1/p62, a cargo receptor that is degraded during autophagy represent the autophagy rate. Hence, we validated our results by assessing the protein levels of LC3BII and p62 as well.

Autophagy determines neural stem cell fate by regulating key signalling pathways like the wnt, and notch. It targets these receptors and degrades them when a cell needs to switch its fate from proliferation to differentiation [29] [24]. Zika virus NS4A and NS4B also enhance the autophagy pathway for replication as reported by us and others [26]. However, the detailed mechanisms of these observations were not explored yet, which necessitated this study to investigate the link between autophagy and NSC proliferation under the effect of ZIKV expression vectors NS4A and NS4B.

Notch signalling regulates several cellular processes like stem cell maintenance, proliferation, fate determination, and apoptosis [41]. Its activated form (NICD) translocates to the nucleus and activates the transcription of target genes such as Hairy-Enhancer of Split (HES) and HES-related proteins (HERP) [41]. These genes repress the transcription of pro-neural genes (e.g. Neurogenin 1, Neurogenin 2) and thereby maintain the NPC proliferation and repress neuronal differentiation. Mutation in HES genes leads to premature differentiation into neurons [42]. Knockdown of notch1 in the embryonic brain leads to a reduction in neural stem cells as well as enhances glial and neuronal differentiation [43]. We analysed the status of the Notch and Wnt signalling in NSCs under the effect of ZIKV expression vectors NS4A and NS4B and observed that the notch signalling was significantly downregulated, as evident from the reduced NICD protein levels. The Notch signalling pathway is an important determinant of NSC fate and has multiple roles in the regulation of NSC differentiation [25]. The phenotype of premature neuronal differentiation is also observed in both Notch1-deficient and RBP-J-deficient mice [43]. To further strengthen the observation that Notch signalling is dysregulated in the ZIKV context, we assessed the expression of HES family genes (Notch targets) that control the commitment of neural stem cells. HES1 and HES5 are known to inhibit neuronal differentiation. These genes may mediate Notch-induced inhibition of cellular development [44]. In Hes1-deficient mice, neurons differentiate prematurely, resulting in severe defects of neural tube formation like anencephaly and abnormalities of the eye [45]. Similarly, in Hes5-deficient mice neurons prematurely differentiate [46]. We found reduced expression of *Hes1 and Hes5* in NSCs after ZIKV NS4A and NS4B co-transfection, which supports the observation of reduced cell proliferation. However, *Hey1* transcript levels remain unaffected. We also observed enhanced transcript levels of neurogenin genes in the co-transfection group. Neurogenins are bHLH transcription factors that promote neurogenesis [47], hence the increased level of neurogenin supports the finding of premature neurogenesis after ZIKV transfection.

To further confirm that the altered NSC fate and notch signalling is mediated by the autophagy pathway, we performed rescue experiments by treating the transfected cells with 3-methyladenine, a well-established autophagy inhibitor. The 3-MA treatment was able to rescue the NS4A + NS4B associated phenotype viz cell proliferation arrest and premature neurogenesis. In future, additional experiments utilizing a loss-of-function approach or siRNA-mediated knockdown of autophagy genes like Beclin-1 can also be performed to further strengthen these findings.

To dissect out the mechanism driving autophagy-mediated alterations in NSC functions under the effect of ZIKV NS4A and NS4B vectors, we focused on mitochondrial processes such as fission and fusion. Mitochondria is the primary source of ROS and ROS in turn directly or indirectly controls autophagy pathways [32]. Further, ROS mediated signalling regulates Neural stem cell proliferation [33]. ROS imbalance and mitochondrial defects have also been observed in iPSC-derived astrocytes following ZIKV transfection, ultimately leading to DNA damage and cell death and ROS scavengers protect these astrocytes by reducing DNA damage. [48]

Our findings suggest that the upregulated mitochondrial phenomena such as mitochondrial fission and ROS production following Zika virus NS4A and NS4B co-transfection, could lead to enhanced autophagy. Literature also suggests that the dysregulated AKT signalling leads to enhanced autophagy after ZIKV infection [26]. AKT signalling is a key event that also regulates mitochondrial dynamics and functionality [49]. Therefore, our finding falls in the same arena and suggests a parallel mechanism of autophagy induction. However more detailed investigation is needed to conclusively link the two findings.

This study concludes that Zika virus NS4A and NS4B alter the neural stem cell fate by arresting their proliferation and diverting them toward premature neurogenesis. These effects are mediated by autophagy that targets the notch pathway and alters the expression of the HES family of genes responsible for regulating proliferation. Downregulating autophagy by 3-MA methyl-adenine attenuates the deleterious effects of NS4A and NS4B by downregulating autophagy and hence enhancing notch expression which then rescues NSCs premature differentiation and maintains NSCs proliferation. In summary, this study reports the role of autophagy in mediating neural stem cell fate determination following ZIKV NS4A and NS4B transfection (Fig. 8), implicating autophagy as a possible line of treatment for Zika virus-induced microcephaly.

Material And Methods

Neural stem cell culture

10–15 weeks old aborted human fetus was collected after informed consent from the mother and the brain tissue was processed to isolate Neural stem cells (NSCs) from the telencephalic region by following the strict guidelines of institutional Human ethics and stem cell research committee of NBRC, India in compliance with recommendations of the Indian Council of Medical Research (ICMR) and Department of Biotechnology (DBT), India. Isolated NSCs were cultured on poly-D-lysine (Sigma Aldrich, Missouri, USA)

coated flasks using neurobasal media supplemented with N2 supplement (Invitrogen, San Diego, CA, USA), Neural survival factor (Lonza, Charles City, IA, USA), glutamine (Sigma, St. Louis, MO, USA), bovine serum albumin (Sigma–Aldrich, St. Louis, MO), 25ng/mL bFGF (Sigma Aldrich, USA), 20ng/mL EGF (Sigma-Aldrich, USA), gentamycin (Sigma, St. Louis, MO, USA) and penicillin and streptomycin solution (Invitrogen, San Diego, CA, USA). These cells were further characterized by immunocytochemistry and western blotting using NSC markers such as (Nestin, and SOX2) and astrocyte and neuronal differentiation markers (GFAP and MAP2 respectively). 99% of cells were found to be positive for Nestin and SOX2 and negative for GFAP and MAP2. Their proliferation efficiency was also confirmed by performing a neurosphere assay and isolated NPCs were found to form good neurospheres.

Transfection

NSCs were seeded at 70–80% confluency and transfected using lipofectamine 3000 (Invitrogen, USA) in opti-MEM (Cat. #31985-070, Invitrogen, CA) media with pCAGIG-IRES-GFF expression vector expressing full-length Zika virus protein NS4A and NS4B using manufacturer's protocol. These plasmids were kindly gifted by Dr. Shyamala Mani (IISc, Bangalore, India). Transfected cells were processed/harvested after 24 or 48h as per experimental requisite. The transfection efficiency of all plasmids in NSCs was found to be comparable (Fig. S3).

Rna And Protein Isolation

Transfected cells were harvested and processed for RNA and Protein isolation by phenol-chloroform extraction principle using TRizol reagent (Ambion, Texas, USA, Cat# 15596018). Briefly, the upper aqueous phase was used to isolate RNA, and the lower PINK organic phase was used to isolate Protein. The RNA pellet was resuspended in Nuclease-free water and concentration was assessed in Nanodrop. The protein pellet was resuspended in SDS lysis buffer that consists of 0.5M Tris pH 7.5, EDTA 0.5 M, NaCl 3 M, NaF 1 M, Na VO 0.5 M, SDS 20% and NaB 100mM and protease inhibitor cocktail (Roche, Mannheim, Germany).

Western Blot

Protein estimation was done using Bicinchonic acid (Sigma) and CuSO₄. Protein samples were resolved on 12% SDS PAGE and transferred onto a Nitrocellulose membrane (MDI, Ambala, India). Blocking was done using 5% skimmed milk (in TBST) after which blots were incubated overnight with the following primary antibodies, LC3B (D11) XP R Rabbit mab CST 3868 (1:1000), mouse SQTm1/p62 ab56416 (1:2000), Rabbit Notch1 ab52627 (1:2000), mouse anti-GAPDH (Santacruz biotech, USA Cat# sc-32233, 1:2000). After 3 washing with TBST the blots were incubated with appropriate secondary antibody conjugated with HRP (Vector Labs, USA, 1:4000) for 1-2h at room temperature followed by 5 washing (5 min each) with 1X TBST. The blots were developed using Chemiluminescent Reagent (Millipore, USA) and

imaged using ChemiGenius Bio-imaging System (Syngene, Cambridge, UK). Image J software (NIH, USA, RRID: SCR_003070) was used for the densitometry analysis of protein bands.

Quantitative Real-time Pcr

cDNA was synthesized from isolated RNA by using High-capacity cDNA Reverse Transcriptase Kit (Applied Biosystems, California, USA, Cat# 4368814) by following manufacturer protocol and Quantitative Real-time PCR (qPCR) was performed in ViiA-7 cycler (ABI, USA, RRID: SCR_019582)) using Power SYBR Green master mix (Applied Biosystems, USA, Cat# 4367659), and manually designed gene-specific primers. The list of primers is in the supplementary table (1). The qPCR cycling conditions used were 95°C for 10 min (1 cycle), 95°C for 20 s, 60°C for 30 s, and 72°C for 40 s (40 cycles).

specificity of primers was confirmed by detecting a single peak in the melt curve analysis.

The data was analyzed using the 2^{-CT} method

Neurosphere Assay

NPCs were seeded in a poly-D-lysine (PDL) coated flask and co-transfected with plasmids encoding ZIKV NS4A and NS4B and vector control for 24 hours using Lipofectamine 3000. After that, cells were trypsinized and again seeded in a non-poly-D-lysine flask. Flask was kept upright in a CO₂ incubator. Images were captured after 48 hours.

At least 5 random images were captured, and neurosphere (n > 300) size was measured by using Image J software (NIH, USA, RRID: SCR_003070), and based on size, they were categorized into three groups, small (size ≤ 50 μm), medium (size 50–100 μm) and large size > 100 μm). percentage of neurospheres in each group was calculated.

Immunocytochemistry

NPCs were seeded in PDL-coated Permanox 8 well chamber slides (Nunc, Kamstrupvej, Denmark) at a density of around 20,000 cells/well. These cells were transfected with ZIKV plasmid encoding NS4A and NS4B for 24 hours. The cells were fixed with 4% paraformaldehyde for 20 mins followed by 3 washes with 1xPBS. The fixed cells were incubated overnight with indicated antibodies. After 14–16 h the cells were washed thrice with 1xPBS and incubated for 1h with secondary antibodies tagged with fluorophore 594 or 488. After 1h, 5 washes with 1xPBS were done and cells were fixed with the Hardset mounting media with DAPI (Vector Labs, USA, Cat# H-1500). Three to five random images were captured in an Axiolmager Z1 microscope (Zeiss, Germany) and analyzed by using Image J software (NIH, USA, RRID: SCR_003070)

Following antibodies were used for Immunocytochemistry

anti-DCX (Abcam, Cambridge, UK, 1:1000), mouse anti- Ki 67 (Millipore, Billerica, USA, 1:1000, Cat# MAB4190, RRID:AB_95092), anti-Nestin (1:1000, Millipore) SOX2 (1:1000, (D6D9)XP Rabbit mAb cell signalling technology (3579S), anti-TUJ-1 (1:2000, Promega, Madison, WI, USA; 1:2000), anti- GFAP (Dako, 1:1000, Cat# Z0334, RRID:AB_10013382)

Cell Death Assay

NPCs were seeded in 8 chambered PDL coated slides (20000 cells/well) and were co-transfected with NS4A and NS4B expression vectors for 24 hours and cells were fixed with 4% Paraformaldehyde for 20 min followed by 3 washes with 1XPBS. Cells were blocked and permeabilized with 4% BSA + 0.01% Triton-X 100 for 1 hour. Terminal deoxynucleotidyl transferase biotin-dUTP nick end labelling (TUNEL) assay was performed Using in situ cell death detection kit TMR-Red (Roche, Switzerland Cat# 12156792910) as per manufacturer's protocol to stain cells undergoing death. Slides were mounted using Hardset mounting media with DAPI (Vector Labs, USA, Cat# H-1500). Axiolmager Z1 microscope (Zeiss, Germany) was used to take random 5 random images per group. Images were analyzed in Image J software (NIH, USA, RRID: SCR_003070)

Ros Detection

Intracellular ROS was measured after transfection with NS4A and NS4B using Cellular ROS Assay Kit (Deep Red ab186029). Briefly, cells were seeded in 24 well plates and transfected for 24 hours. After 24 hours the media was changed with fresh media containing ROS deep red dye and incubated for 30 min in an incubator at 37°C, after 30 min the cells were washed with PBS. changes in fluorescence intensity (Ex/m = 650/675 nm) were measured using Tecan infinite PRO 200.

Drug Treatment

Cells were co-transfected with ZIKV NS4A and NS4B expression vector using Lipofectamine 3000 in Opti-MEM media, after 12h of transfection 3 methyladenine (3.5uM) drug was added. Milli-Q was used as drug control. The cells were harvested after 24 h and processed for other assays.

Statistical analysis

All the experiments were performed/repeated three to five times independently as specified in the legends. Results were represented as mean \pm SD. Student's t-test was performed for experiments having only one variable whereas one-way ANOVA was performed for multiple groups to determine the significance of the means. P values < 0.05 were considered statistically significant. * Represents $p < 0.05$, ** $p < 0.005$, and *** $p < 0.0005$.

Declarations

Acknowledgment

We acknowledge the technical assistance from Mr. Naushad Alam and Mr. DL Meena of NBRC. Mr. Naushad also helped in performing some assays. We are thankful to Dr. Shyamala Mani, IISc, India for providing Expression vectors for the Zika virus proteins. We highly acknowledge the fellowship from Council of Scientific and Industrial Research (CSIR) to Bindu and Hriday Shanker Pandey and financial support from NBRC core funds to Prof. Pankaj Seth. We also acknowledge the support of the facilities provided under the Biotechnology Information System Network (BTISNET) grant, Department of Biotechnology (DBT), India, and Distributed Information Centre at NBRC, Manesar, India.

Statement and Declaration

Funding

This study was supported by Council of Scientific and Industrial Research, Department of Biotechnology (DBT) and National Brain Research Centre (NBRC) core fund.

Competing interest

The authors declare no competing interests.

Author Contributions

Bindu designed the study, performed experiments, analyzed the data, and wrote the manuscript. Hriday Shanker Pandey helped in performing rescue experiments and writing the manuscript. Pankaj Seth helped in designing experiments, interpretation of data, and finalizing the manuscript.

Data Availability

All data generated during this study are available from the corresponding author on reasonable request.

Ethical approval

Strict guidelines of institutional Human ethics and stem cell research committee of NBRC, India in compliance with recommendations of the Indian Council of Medical Research (ICMR) and Department of Biotechnology (DBT), India were followed for isolation of Neural stem cells from aborted human fetus.

Consent to participate

Not applicable

Consent to publish

Not applicable

References

1. Wen Z, Song H, Ming G (2017) How does Zika virus cause microcephaly? *Genes Dev* 31:849–861. <https://doi.org/10.1101/gad.298216.117>
2. Ss P et al (2017) Overview on the Current Status of Zika Virus Pathogenesis and Animal Related Research. *J neuroimmune pharmacology: official J Soc NeuroImmune Pharmacol* 12. <https://doi.org/10.1007/s11481-017-9743-8>
3. Miner JJ, Diamond MS (2017) Zika Virus Pathogenesis and Tissue Tropism. *Cell Host Microbe* 21:134–142. <https://doi.org/10.1016/j.chom.2017.01.004>
4. Mlakar J, Korva M, Tul N et al (2016) Zika Virus Associated with Microcephaly. *N Engl J Med* 374:951–958. <https://doi.org/10.1056/NEJMoa1600651>
5. Carteaux G, Maquart M, Bedet A et al (2016) Zika Virus Associated with Meningoencephalitis. *N Engl J Med* 374:1595–1596. <https://doi.org/10.1056/NEJMc1602964>
6. Mécharles S, Herrmann C, Poullain P et al (2016) Acute myelitis due to Zika virus infection. *The Lancet* 387:1481. [https://doi.org/10.1016/S0140-6736\(16\)00644-9](https://doi.org/10.1016/S0140-6736(16)00644-9)
7. Styczynski AR, Malta JMAS, Krow-Lucal ER et al (2017) Increased rates of Guillain-Barré syndrome associated with Zika virus outbreak in the Salvador metropolitan area, Brazil. *PLoS Negl Trop Dis* 11:e0005869. <https://doi.org/10.1371/journal.pntd.0005869>
8. Xu D, Li C, Qin C-F, Xu Z (2019) Update on the Animal Models and Underlying Mechanisms for ZIKV-Induced Microcephaly. *Annu Rev Virol* 6:459–479. <https://doi.org/10.1146/annurev-virology-092818-015740>
9. Barbelanne M, Tsang WY (2014) Molecular and Cellular Basis of Autosomal Recessive Primary Microcephaly. *Biomed Res Int* 2014:547986. <https://doi.org/10.1155/2014/547986>
10. McDonnell LM, Warman Chardon J, Schwartzenruber J et al (2014) The utility of exome sequencing for genetic diagnosis in a familial microcephaly epilepsy syndrome. *BMC Neurol* 14:22. <https://doi.org/10.1186/1471-2377-14-22>
11. Tanaka AJ, Cho MT, Millan F et al (2015) Mutations in SPATA5 Are Associated with Microcephaly, Intellectual Disability, Seizures, and Hearing Loss. *Am J Hum Genet* 97:457–464. <https://doi.org/10.1016/j.ajhg.2015.07.014>
12. Merfeld E, Ben-Avi L, Kennon M, Cervený KL (2017) Potential mechanisms of Zika-linked microcephaly. *Wiley Interdiscip Rev Dev Biol* 6:e273. <https://doi.org/10.1002/wdev.273>
13. Garcez PP, Loiola EC, Madeiro da Costa R et al (2016) Zika virus impairs growth in human neurospheres and brain organoids. *Science* 352:816–818. <https://doi.org/10.1126/science.aaf6116>
14. Qian X, Nguyen HN, Song MM et al (2016) Brain-Region-Specific Organoids Using Mini-bioreactors for Modeling ZIKV Exposure. *Cell* 165:1238–1254. <https://doi.org/10.1016/j.cell.2016.04.032>
15. Tang H, Hammack C, Ogden SC et al (2016) Zika Virus Infects Human Cortical Neural Progenitors and Attenuates Their Growth. *Cell Stem Cell* 18:587–590. <https://doi.org/10.1016/j.stem.2016.02.016>

16. Li C, Xu D, Ye Q et al (2016) Zika Virus Disrupts Neural Progenitor Development and Leads to Microcephaly in Mice. *Cell Stem Cell* 19:120–126. <https://doi.org/10.1016/j.stem.2016.04.017>
17. Shao Q, Herrlinger S, Yang S-L et al (2016) Zika virus infection disrupts neurovascular development and results in postnatal microcephaly with brain damage. *Development* 143:4127–4136. <https://doi.org/10.1242/dev.143768>
18. Wu K-Y, Zuo G-L, Li X-F et al (2016) Vertical transmission of Zika virus targeting the radial glial cells affects cortex development of offspring mice. *Cell Res* 26:645–654. <https://doi.org/10.1038/cr.2016.58>
19. Yuan L, Huang X-Y, Liu Z-Y et al (2017) A single mutation in the prM protein of Zika virus contributes to fetal microcephaly. *Science* 358:933–936. <https://doi.org/10.1126/science.aam7120>
20. Bhagat R, Prajapati B, Narwal S et al (2018) Zika virus E protein alters the properties of human fetal neural stem cells by modulating microRNA circuitry. *Cell Death Differ* 25:1837–1854. <https://doi.org/10.1038/s41418-018-0163-y>
21. Cugola FR, Fernandes IR, Russo FB et al (2016) The Brazilian Zika virus strain causes birth defects in experimental models. *Nature* 534:267–271. <https://doi.org/10.1038/nature18296>
22. Goodfellow FT, Willard KA, Wu X et al (2018) Strain-Dependent Consequences of Zika Virus Infection and Differential Impact on Neural Development. *Viruses* 10:E550. <https://doi.org/10.3390/v10100550>
23. Liang Q, Luo Z, Zeng J et al (2016) Zika Virus NS4A and NS4B Proteins Deregulate Akt-mTOR Signaling in Human Fetal Neural Stem Cells to Inhibit Neurogenesis and Induce Autophagy. *Cell Stem Cell* 19:663–671. <https://doi.org/10.1016/j.stem.2016.07.019>
24. Wu X, Fleming A, Ricketts T et al (2016) Autophagy regulates Notch degradation and modulates stem cell development and neurogenesis. *Nat Commun* 7:10533. <https://doi.org/10.1038/ncomms10533>
25. Venkatesh K, Reddy LVK, Abbas S et al (2017) NOTCH Signaling Is Essential for Maturation, Self-Renewal, and Tri-Differentiation of In Vitro Derived Human Neural Stem Cells. *Cell Reprogram* 19:372–383. <https://doi.org/10.1089/cell.2017.0009>
26. Liang Q, Luo Z, Zeng J et al (2016) Zika Virus NS4A and NS4B Proteins Deregulate Akt-mTOR Signaling in Human Fetal Neural Stem Cells to Inhibit Neurogenesis and Induce Autophagy. *Cell Stem Cell* 19:663–671. <https://doi.org/10.1016/j.stem.2016.07.019>
27. Dong X, Levine B (2013) Autophagy and Viruses: Adversaries or Allies? *J Innate Immun* 5:480–493. <https://doi.org/10.1159/000346388>
28. Barth S, Glick D, Macleod KF (2010) Autophagy: assays and artifacts. *J Pathol* 221:117–124. <https://doi.org/10.1002/path.2694>
29. Gao C, Cao W, Bao L et al (2010) Autophagy negatively regulates Wnt signalling by promoting Dishevelled degradation. *Nat Cell Biol* 12:781–790. <https://doi.org/10.1038/ncb2082>
30. Zhou Z-D, Kumari U, Xiao Z-C, Tan E-K (2010) Notch as a molecular switch in neural stem cells. *IUBMB Life* 62:618–623. <https://doi.org/10.1002/iub.362>

31. Wu Y-T, Tan H-L, Shui G et al (2010) Dual Role of 3-Methyladenine in Modulation of Autophagy via Different Temporal Patterns of Inhibition on Class I and III Phosphoinositide 3-Kinase. *J Biol Chem* 285:10850–10861. <https://doi.org/10.1074/jbc.M109.080796>
32. Scherz-Shouval R, Elazar Z (2011) Regulation of autophagy by ROS: physiology and pathology. *Trends Biochem Sci* 36:30–38. <https://doi.org/10.1016/j.tibs.2010.07.007>
33. Khacho M, Clark A, Svoboda DS et al (2016) Mitochondrial Dynamics Impacts Stem Cell Identity and Fate Decisions by Regulating a Nuclear Transcriptional Program. *Cell Stem Cell* 19:232–247. <https://doi.org/10.1016/j.stem.2016.04.015>
34. Marbán-Castro E, Goncé A, Fumadó V et al (2021) Zika virus infection in pregnant women and their children: A review. *Eur J Obstet Gynecol Reprod Biol* 265:162–168. <https://doi.org/10.1016/j.ejogrb.2021.07.012>
35. Dang JW, Tiwari SK, Qin Y, Rana TM (2019) Genome-wide Integrative Analysis of Zika-Virus-Infected Neuronal Stem Cells Reveals Roles for MicroRNAs in Cell Cycle and Stemness. *Cell Rep* 27:3618–3628e5. <https://doi.org/10.1016/j.celrep.2019.05.059>
36. Rothan HA, Fang S, Mahesh M, Byrareddy SN (2019) Zika Virus and the Metabolism of Neuronal Cells. *Mol Neurobiol* 56:2551–2557. <https://doi.org/10.1007/s12035-018-1263-x>
37. Garza-Lombó C, Gonsebatt ME (2016) Mammalian Target of Rapamycin: Its Role in Early Neural Development and in Adult and Aged Brain Function. *Frontiers in Cellular Neuroscience* 10
38. Phan TP, Holland AJ (2021) Time is of the essence: the molecular mechanisms of primary microcephaly. *Genes Dev* 35:1551–1578. <https://doi.org/10.1101/gad.348866.121>
39. Sotthibundhu A, Promjuntuek W, Liu M et al (2018) Roles of autophagy in controlling stem cell identity: a perspective of self-renewal and differentiation. *Cell Tissue Res* 374:205–216. <https://doi.org/10.1007/s00441-018-2829-7>
40. Eskelinen E-L (2006) Roles of LAMP-1 and LAMP-2 in lysosome biogenesis and autophagy. *Mol Aspects Med* 27:495–502. <https://doi.org/10.1016/j.mam.2006.08.005>
41. Lasky JL, Wu H (2005) Notch signaling, brain development, and human disease. *Pediatr Res* 57. <https://doi.org/10.1203/01.PDR.0000159632.70510.3D>. :104R-109R
42. Ohtsuka T, Ishibashi M, Gradwohl G et al (1999) Hes1 and Hes5 as notch effectors in mammalian neuronal differentiation. *EMBO J* 18:2196–2207. <https://doi.org/10.1093/emboj/18.8.2196>
43. de la Pompa JL, Wakeham A, Correia KM et al (1997) Conservation of the Notch signalling pathway in mammalian neurogenesis. *Development* 124:1139–1148. <https://doi.org/10.1242/dev.124.6.1139>
44. Kageyama R, Ohtsuka T (1999) The Notch-Hes pathway in mammalian neural development. *Cell Res* 9:179–188. <https://doi.org/10.1038/sj.cr.7290016>
45. Tomita K, Ishibashi M, Nakahara K et al (1996) Mammalian hairy and Enhancer of split homolog 1 regulates differentiation of retinal neurons and is essential for eye morphogenesis. *Neuron* 16:723–734. [https://doi.org/10.1016/s0896-6273\(00\)80093-8](https://doi.org/10.1016/s0896-6273(00)80093-8)

46. Ishibashi M, Ang SL, Shiota K et al (1995) Targeted disruption of mammalian hairy and Enhancer of split homolog-1 (HES-1) leads to up-regulation of neural helix-loop-helix factors, premature neurogenesis, and severe neural tube defects. *Genes Dev* 9:3136–3148. <https://doi.org/10.1101/gad.9.24.3136>
47. Imayoshi I, Kageyama R (2014) bHLH factors in self-renewal, multipotency, and fate choice of neural progenitor cells. *Neuron* 82:9–23. <https://doi.org/10.1016/j.neuron.2014.03.018>
48. Zika virus infection leads to mitochondrial failure, oxidative stress and DNA damage in human iPSC-derived astrocytes | *Scientific Reports*. <https://www.nature.com/articles/s41598-020-57914-x>. Accessed 28 Dec 2022
49. Xie X, Shu R, Yu C et al (2022) Mammalian AKT, the Emerging Roles on Mitochondrial Function in Diseases. *Aging Dis* 13:157–174. <https://doi.org/10.14336/AD.2021.0729>

Figures

Fig. 1

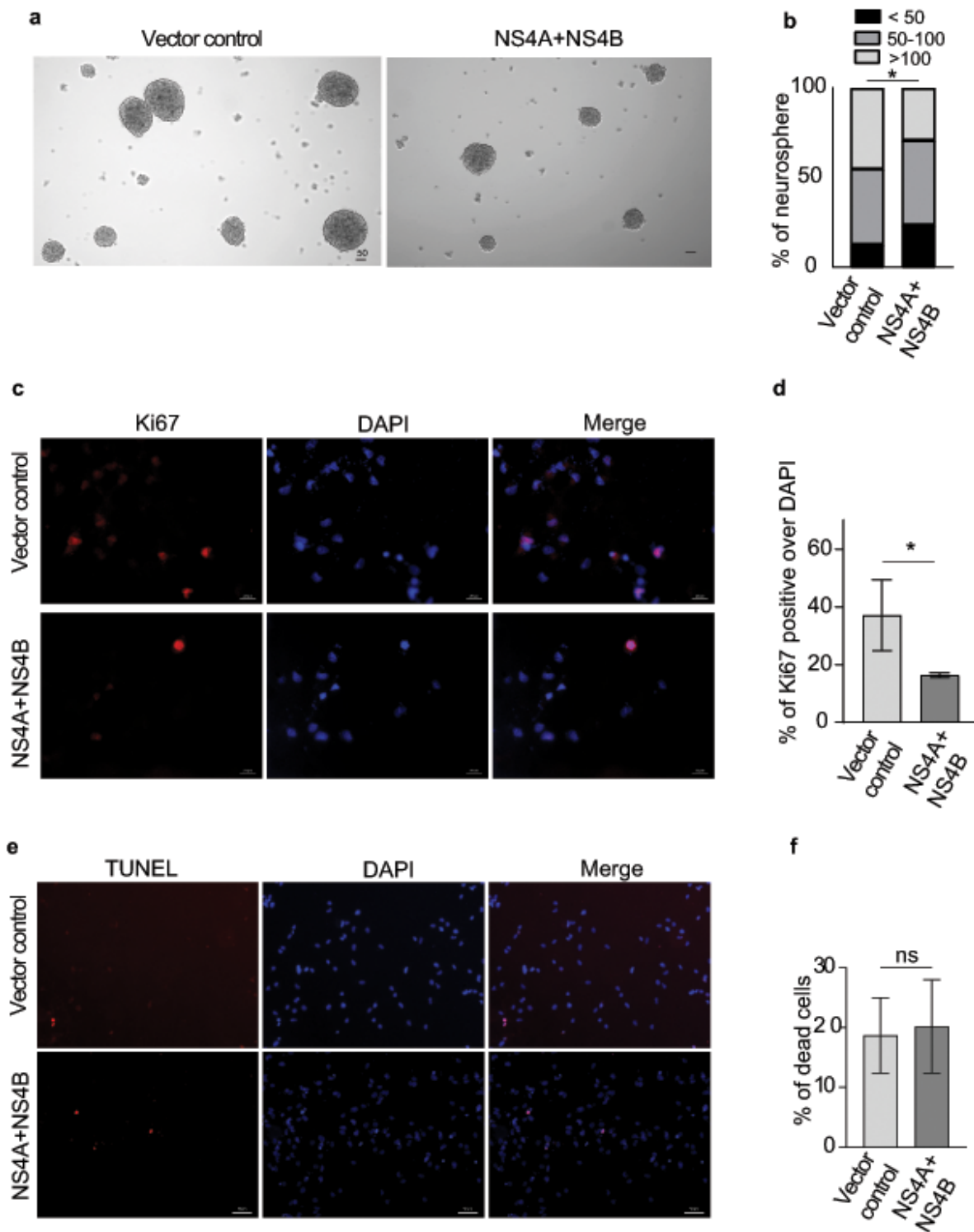


Figure 1

Zika virus (ZIKV) protein NS4A-NS4B reduces human fetal neural stem cell (fNSC) proliferation without altering survival. **(a)** Neural stem cells were isolated from the SV region of the aborted fetus following ethical guidelines. These cells express well-established markers SOX2 and DCX. fNSCs were co-transfected with NS4A and NS4B for 24 h and proliferation was assessed by performing neurosphere formation assay and ki67 immunolabeling. Neurospheres were analyzed 48 h after the 24h of NS4A and

NS4B co-transfection. Representative bright field images showing compromised neurospheres after ZIKV transfection. Scale -50 μm . **(b)** Bar graph showing neurosphere size distribution in vector control and NS4A-NS4B transfected group. **(c)** Immunocytochemistry images showing proliferation marker ki67 (red) and DAPI (blue) for the nucleus after 24 h of transfection with vector control and NS4A-NS4B combination. scale 20 μm . **(d)** Bar graph representing the percentage of ki67 positive cells over DAPI. **(e)** Immunocytochemistry images showing TUNEL positive cells (red) and DAPI (blue) for nucleus after transfection with indicated groups control vector or combination of NS4A and NS4B for 24 h to check cell survival. scale 50 μm . **(f)** Bar graph representing the percentage of TUNEL-positive cells over DAPI. The values represent the mean \pm standard deviation. V- empty vector, NS4A +NS4B – Co-transfection of vectors containing ZIKV non-structural protein 4A and 4B). N=3-5 (Independent replicates). Statistics, for B, * $p < 0.05$, Chi-square test and for D, F, * $p < 0.05$, unpaired t-test.; ns, not significant.

Fig. 2

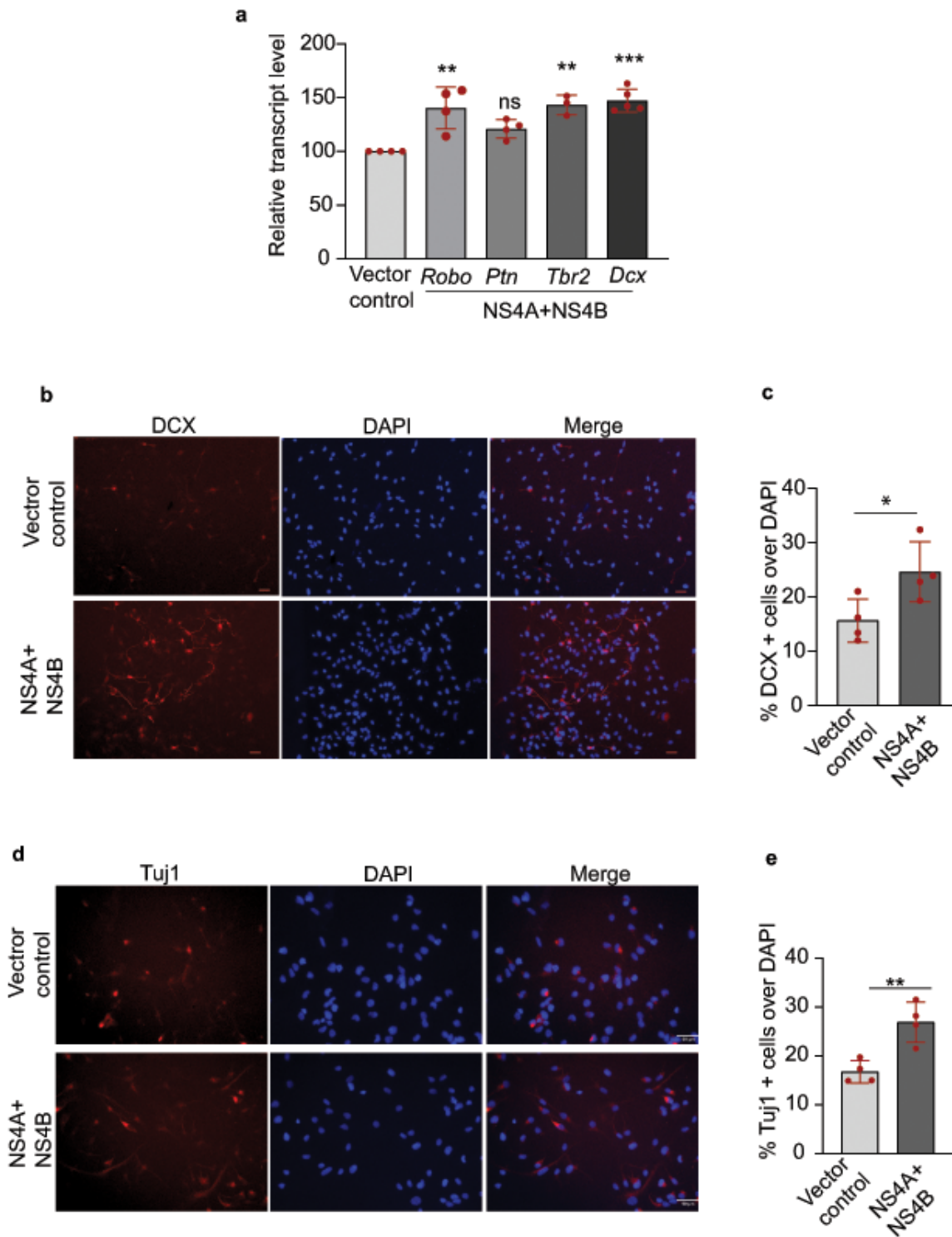


Figure 2

ZIKA virus protein NS4A-NS4B protein induces premature neurogenesis of fNSCs. **(a)** Human fNSCs were co-transfected with NS4A and NS4B for 24 h and neurogenesis was evaluated in non-differentiating culture condition. Bar graph representing relative mRNA expression of neurogenic genes or pro-neural genes DCX, Robo, PTN, and neural progenitor commitment gene Tbr2 normalized with Gapdh at 24h post-transfection with control Vector or vector containing NS4A - NS4B. **(b)** Representative images showing

Immunocytochemistry labeling of early neurogenesis marker DCX (red) and nucleus (DAPI). Scale 50 μm . **(c)** Quantification of DCX positive cells over DAPI for vector control and Co-transfection group. **(d)** Immunocytochemistry images after transfection with NS4A and NS4B showing immature neurogenesis marker TUJ1 (Red) and DAPI (blue) staining nucleus. Scale 50 μm . **(e)** Bar graph representing fold change in TUJ1 positive cells over DAPI. The values represent the mean \pm standard deviation. V- empty vector, NS4A+NS4B- Co-transfection of vectors containing ZIKV non-structural protein 4A and 4B. N=3-5 (Independent replicates). Statistics, for A, C, E * $p < 0.05$, ** $p < 0.01$, *** $p < 0.001$; unpaired t-test.; ns, not significant.

Fig. 3

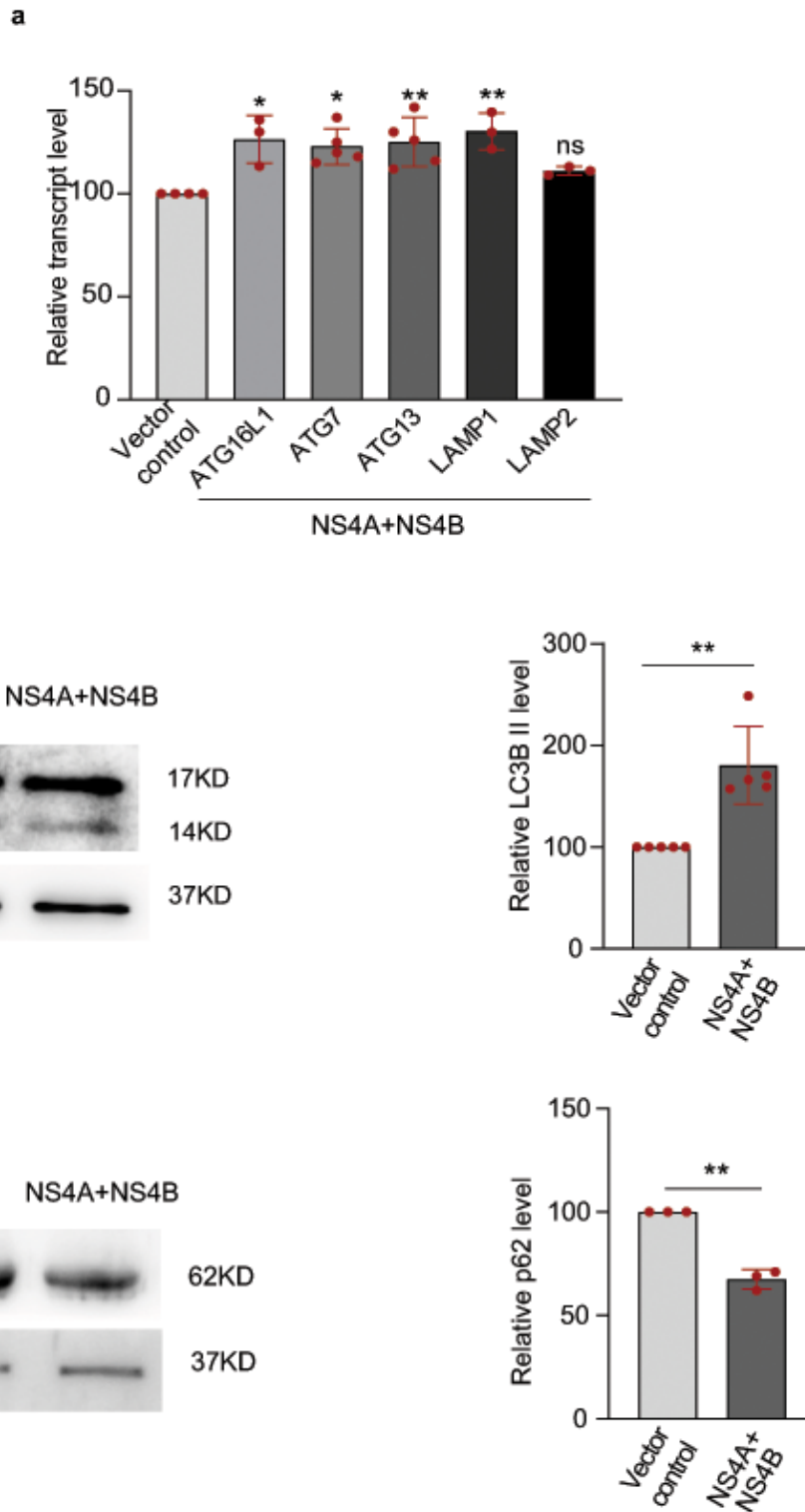


Figure 3

ZIKV NS4A-NS4B co-transfection induces autophagy in fNSCs. **(a)** fNSCs were co-transfected with ZIKV NS4A and NS4B plasmids and after 24 h mRNA expression of autophagic genes was evaluated. Bar graph showing relative mRNA expression of autophagy genes (*atg7*, *atg16L1*, *atg13*) and Lysosomal markers (*Lamp1* and *Lamp2*), *Gapdh* was used as the normalization control. **(b)** Immunoblots showing increased LC3BII (autophagosome formation reporter) level after co-transfection with NS4A-NS4B

compared to vector control. Left panel showing representative blots and the right panel showing a bar graph of the densitometry analysis of blots. (c) Immunoblots showing decreased p62 (autophagy rate reporter) level after co-transfection with NS4A-NS4B compared to vector control. Left panel showing representative blots and the Right panel showing a bar graph of the densitometry analysis of blots. V- empty vector, NS4A +NS4B – Co-transfection of the vector containing ZIKV non-structural protein 4A and 4B. N=3-5 (Independent replicates). Statistics, for A, B, C * $p < 0.05$, ** $p < 0.01$, unpaired t-test.; ns- not significant.

Fig. 4

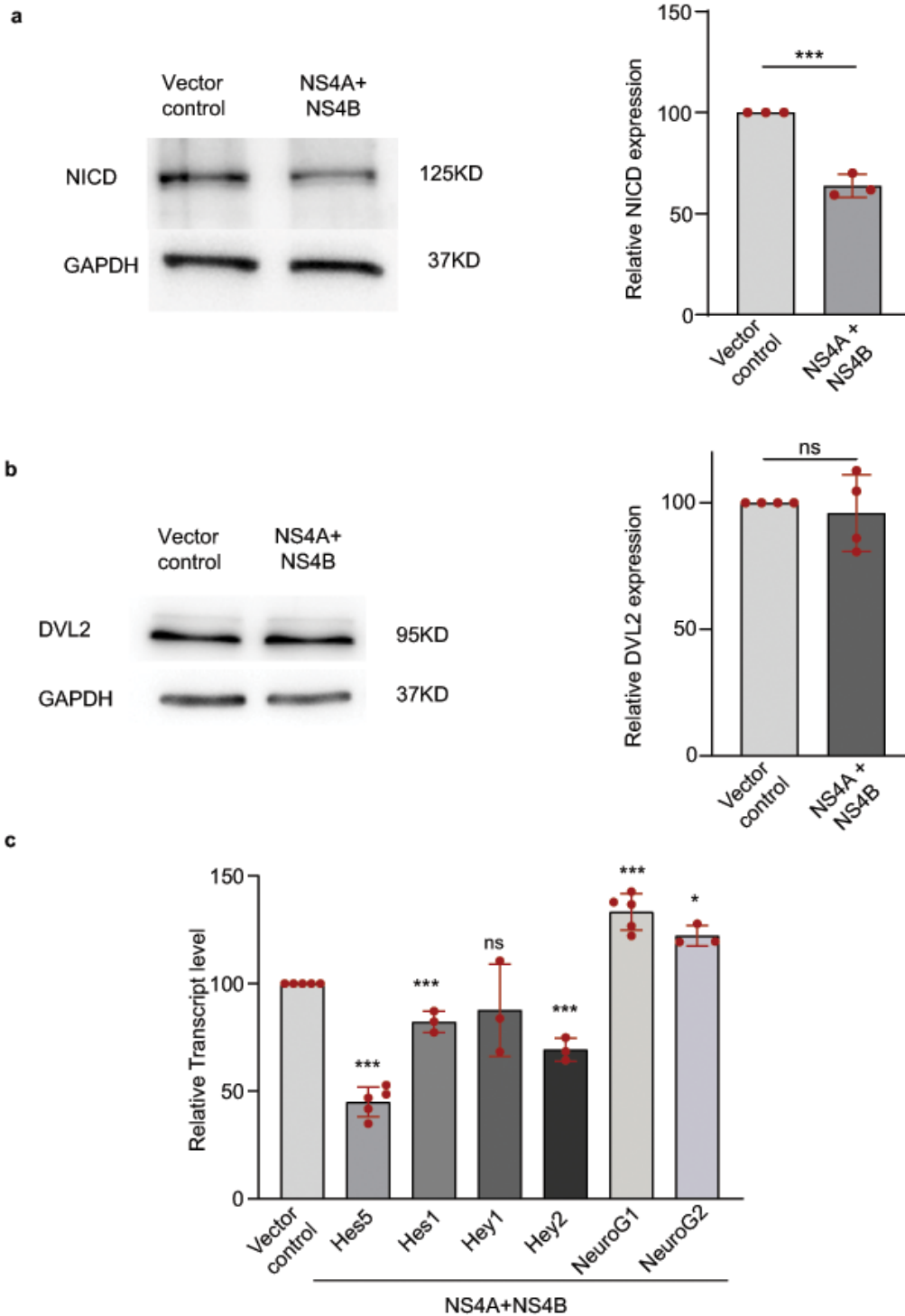


Figure 4

ZIKV NS4A - NS4B protein downregulates the notch pathway in fNSCs. fNSCs were co-transfected with NS4A and NS4B for 24 h and subjected to immunoblot and quantitative PCR analysis. **(a)** Immunoblots showing decreased NICD (Notch1) level after co-transfection with NS4A-NS4B compared to vector control. Left panel showing representative blots and the right panel showing a bar graph of the densitometry analysis of blots. GAPDH was used as the normalization control. **(b)** Representing images of immunoblotting with DVL2 (wnt receptor) specific antibody (left panel) and its quantification (right panel). GAPDH was used as the normalization control. **(c)** Bar graph showing relative mRNA expression of NOTCH1 target genes *Hes1*, *Hes5*, *Hey1*, *Hey2*, Neurogenin1, and Neurogenin 2 after co-transfection. *Gapdh* was used as the Normalization control. V- empty vector, NS4A +NS4B – Co-transfection of the vector containing ZIKV non-structural protein 4A and 4B). N=3-5 (Independent replicates). Statistics, for A, B, C * $p < 0.05$, *** $p < 0.001$, unpaired t-test.; ns, not significant.

Fig. 5

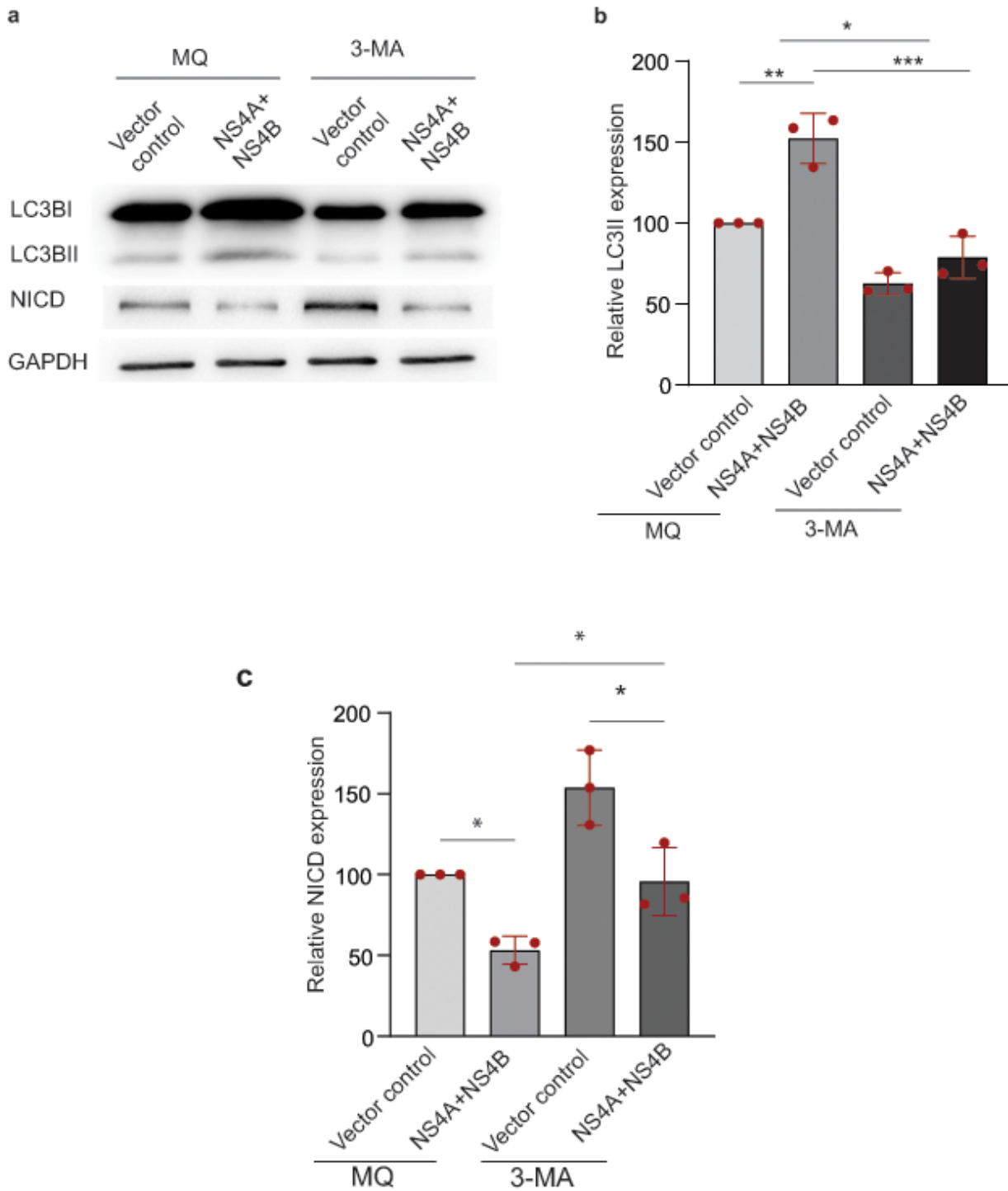


Figure 5

Downregulation of the Autophagy pathway enhances notch1 protein expression in NS4A NS4B transfected group. fNSCs were co-transfected with ZIKV NS4A and NS4B for 12 h followed by autophagy inhibitor 3 methyladenine (3.5 μ M) treatment for 12h. After 24 h post-transfection, the cells were harvested for immunoblot analysis. **(a)** Representing images of immunoblots showing LC3BII and NICD levels after drug treatment post-transfection. GAPDH was used as the normalization control. **(b)** The bar

graph showing densitometry quantification represents reduced LC3BII levels after 3-MA treatments following ZIKV protein transfection. (c) The bar graph showing densitometry quantification represents increased NICD levels after 3-MA treatment following ZIKV protein transfection. 3-MA- 3 methyladenine, V- empty vector, and NS4A +NS4B – Co-transfection of the vector containing ZIKV non-structural protein 4A and 4B.N=3-5 (Independent replicates). Statistics, for B, C, * $p < 0.05$, ** $p < 0.01$, *** $p < 0.001$ ANOVA with Tukey's multiple comparison test.; ns, not significant.

Fig.6

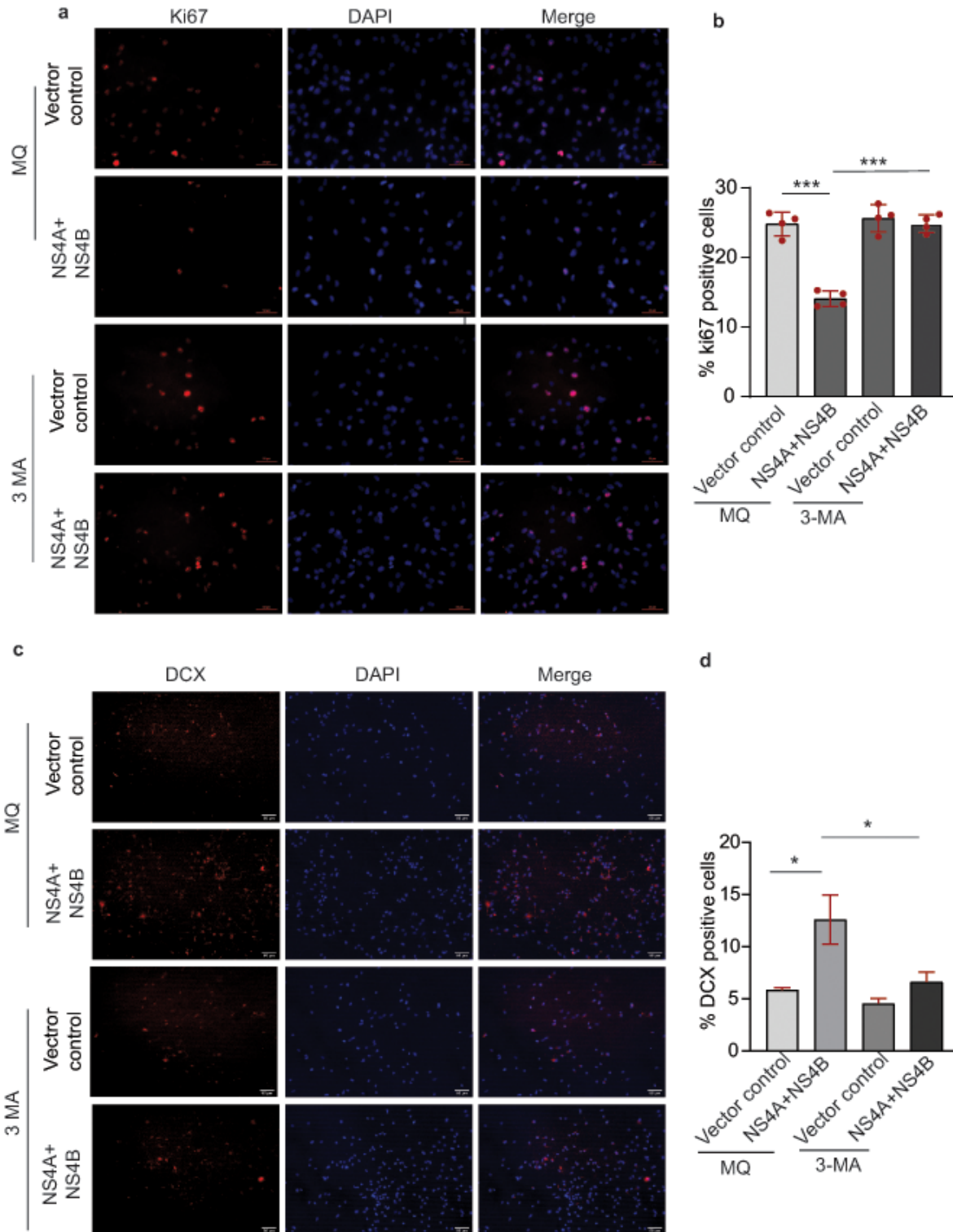


Figure 6

Downregulation of Autophagy induces NSC Proliferation and reduces premature neurogenesis in ZIKV NS4A- NS4B co-transfected fNSCs. fNSCs were co-transfected with ZIKV NS4A and NS4B for 12 h followed by autophagy inhibitor 3-MA (3.5 μ M) treatment for 12h. After 24 h post-transfection, the cells were subjected to Immunocytochemistry analysis. **(a)** Immunocytochemistry images showing proliferation marker ki67 (red) and DAPI (blue) for the nucleus. Scale 50 μ m. **(b)** Bar graph showing increased ki67 positive cells after 3-MA treatment following ZIKV protein transfection. **(c)** Representative images showing Immunocytochemistry labeling of early neurogenesis marker DCX (red) and nucleus (DAPI). Scale 50 μ m. **(d)** Bar graph showing reduced DCX positive cells after 3-MA treatment following ZIKV protein transfection. 3-MA- 3 methyladenine, V- empty vector, and NS4A +NS4B – Co-transfection of the vector containing ZIKV non-structural protein 4A and 4B. N=3-5 (Independent replicates). Statistics, for B, D, *p < 0.05, **p < 0.01, ***p < 0.001 ANOVA with Tukey's multiple comparison test; ns, not significant.

Fig. 7

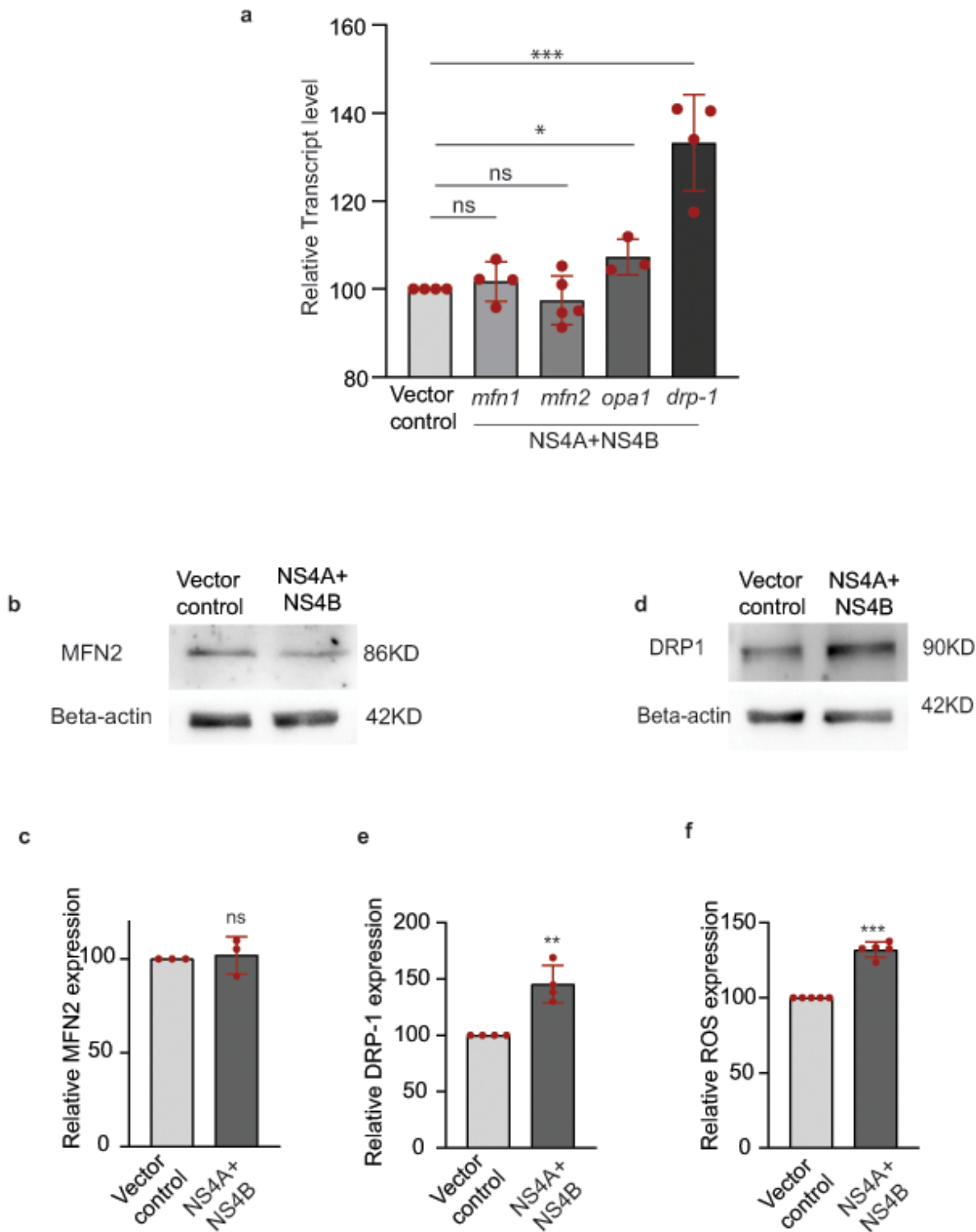


Figure 7

Altered mitochondrial dynamics following ZIKV NS4A - NS4B co-transfection. fNSCs were co-transfected with NS4A and NS4B, and after 24 hours the cells were analyzed for evaluating mitochondrial dynamics and ROS production. **(a)** Bar graph showing relative mRNA expression of mitochondrial fusion (*Mfn1*, *Mfn2*, *Opa1*) and mitochondrial fission gene (*Drp1*) genes normalized with *Gapdh* after 24h post-transfection with vector control or vector encoding NS4A and NS4B. **(b)** Representing images of

immunoblots showing MFN2 levels after co-transfection and its quantification (c). (d) Representing images of immunoblots showing DRP1 levels after co-transfection and its quantification (e). Beta-actin was used as the normalization control. (f) Bar graph showing increased ROS production after NS4A-NS4B co-transfection compared to vector control. V- empty vector, and NS4A +NS4B – Co-transfection of the vector containing ZIKV non-structural protein 4A and 4B. N=3-5 (Independent replicates). Statistics, for A, C, F, *p < 0.05, **p < 0.01, ***p < 0.001; unpaired t-test.; ns, not significant.

Fig. 8

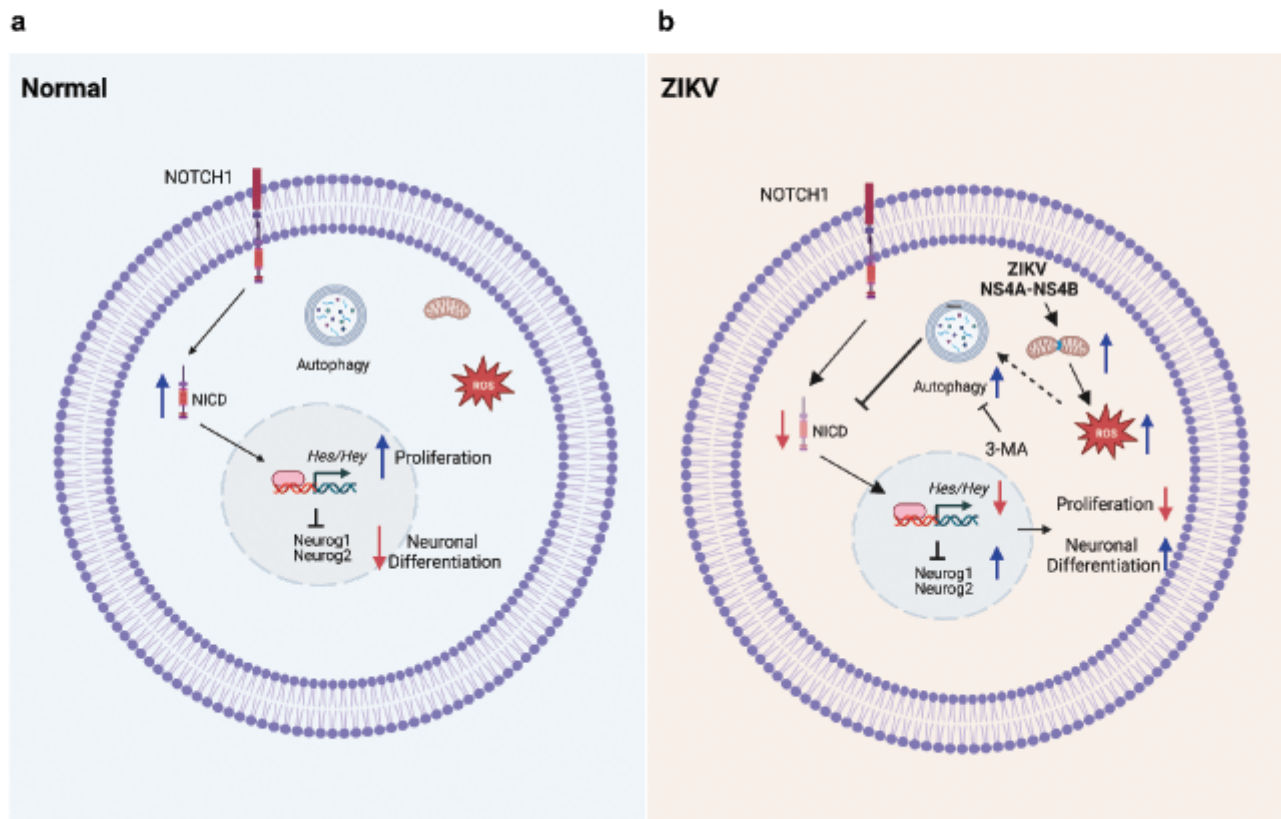


Figure 8

Schematics representing the role of zika virus protein NS4A and NS4B in altered neural stem cell fate.(a) In normal basal autophagy and ROS condition, the notch receptor gets activated and NICD translocate to the nucleus where it activates *hes/ hey* family of genes which maintains the proliferation of NSCs and inhibit premature differentiation by repressing proneural genes (*neurog1, neurog2*).(b)ZIKV protein NS4A and NS4B probably induce mitochondrial fission leading to enhanced ROS production which induces autophagy leading to NICD degradation. So, expression of *hes/hey* family of genes decrease leading to reduced proliferation and expression of proneural genes resulting in premature differentiation of neural

stem cells into the neuron and hence reducing the pool of neural stem cells. Schematics is created using Biorender.

Supplementary Files

This is a list of supplementary files associated with this preprint. Click to download.

- [Supplimentary.pdf](#)